Application of Precast RC Slab Pavements at Airports

Yoshitaka Hachiya[1], Akihiko Ito[2] and Hideki Tanaka[3]

Abstract

Concrete pavements are generally used for airport aprons. Recently, concrete has often been applied also to taxiways in response to the recent introduction of larger aircraft and increased aircraft operations. As a practical measure for constructing concrete pavements without the need to close the facilities, the precast prestressed concrete slab pavement has been used hitherto. However, certain problems with this system, such as jointing system and construction cost, have been noted. This study seeks to overcome these problems by introducing a pavement system using precast reinforced concrete (PRC) slabs using high-strength concrete with cotter joints. First, both the PRC slab and cotter joint were analyzed using Westergaard's formula and a finite element method, and then the system was examined experimentally with small specimens. Design principles for both the PRC slabs and cotter joints were then developed. Finally, experimental pavements were constructed with several PRC slabs and cotter joints, and the repetitive loading tests with B747 landing gear were conducted. The durability of both the PRC slab and the cotter joint were verified through the loading test. On the basis of this work, a structural design procedure for PRC slab pavements at airports was established.

Introduction

With increasing aircraft size and traffic volumes, airport pavements often need repairs. Ground subsidence is also a common problem, as many airports have been built on soft, reclaimed ground in Japan. When repairs are required, it is necessary to complete the work as rapidly as possible.

The need to complete work quickly led to development of a repair method for airport aprons using precast prestressed concrete (PPC) slabs (Sato et al. 1981). The slabs are prepared in the factory, transported to the site, laid on the subbase, and then connected to neighboring slabs. The so-called horn joint system, using horn-shaped reinforcing steels, has been used to allow replacement of damaged slabs only, but this can lead to distress such as pumping at the joints. The compression joint, in which adjacent slabs are held together with compressive force applied through PC tendons, has been developed to solve this difficulty. This type of PPC slab pavement has been adopted at many airports, and the compression joint is confirmed to provide better performance (Hachiya et al. 2001). However, there is a need to reduce the cost of both construction and repair.

---

[1] Dr. Eng., National Institute for Land and Infrastructure Management, Ministry of Land, Infrastructure and Transport, 1-1, Nagase 3, Yokosuka 239-0826, Japan, e-mail: hachiya@ipc.ysk.nilim.go.jp
[2] GAEART TK Co., Ltd., 8-27, Ogawa-cho, Shinjuku, Tokyo 162-0814, Japan, e-mail: aitou@gaeart.com
[3] GEOSTR Corporation, 17-8, Nishikata 1, Bunkyo, Tokyo 113-0024, Japan, e-mail: tanaka-hideki@geostr.co.jp

This new study was begun with the aim of reducing the troublesome work of slab production and slab connection, and to improve load-transfer efficiency at the joint. The subject of the study is a precast reinforced concrete slab system using high-strength concrete (PRC slabs) and so-called cotter joints as connections. If effective, this system would certainly meet the requirement for cost reduction.

In the study, a PRC slab pavement designed for airports was constructed experimentally and load-tested with repeated large aircraft loading. Both the slab structure and cotter joint system were examined. This paper explains the study procedure and summarizes the applicability of PRC slab pavements to airports.

High-strength PRC slab pavement

The PRC slab pavement consists of linked PRC slabs resting on the subbase. PRC slab rigidity is secured by the use of Portland cement concrete with higher strength and lattice truss-shaped reinforcement, as shown in Photo 1. To connect the PRC slabs together, a cotter joint system is used.

The basic construction method for a PRC slab pavement is as follows: first, the existing concrete slab is removed and a cement-stabilized subbase is prepared. The sides of remaining slabs are drilled for the installation of tie bars, if necessary. Next, after laying a plastic film over the subbase, PRC slabs are placed in pre-determined positions. At this time, level differences between adjoining slabs and joint openings are adjusted. Then, after connecting the PRC slabs temporarily, openings at joints and voids beneath the slabs are grouted with cement slurry. Finally, once the cement slurry has hardened, the H-shaped wedges are inserted into the C-shaped cups of the cotter joints and tightened using through-bolts. To finish, both the cotter joints and the grout injection holes are capped.

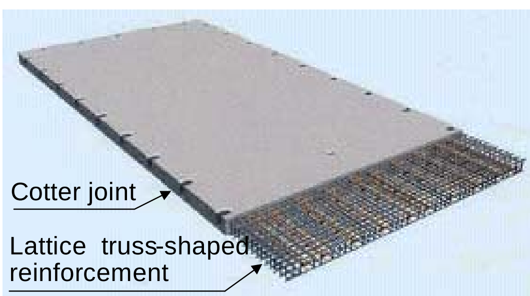

a) PRC slab

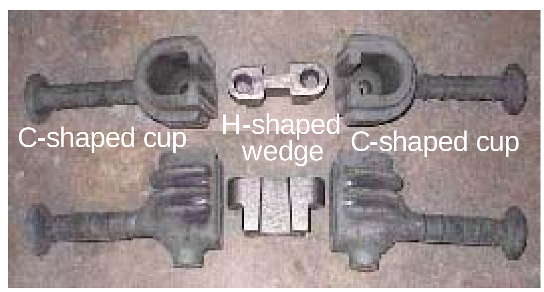

b) Cotter joint system

Photo 1. PRC slab pavement.

Study objectives

The applicability of PRC slab pavements to airports was verified by ensuring that the requirements laid out in the following paragraphs are met. To do this, a series of experiments consisting of both laboratory tests and loading tests on an experimental pavement were planned.

PRC slab. The PRC slab is a reinforced concrete slab in which reinforcing steels are arranged in upper and lower portions, and a Portland cement concrete with high compressive strength of 60 MPa is used. The structural design should comply with that for PPC slabs described in the design principles for airport pavements (MOLIT 2001). Namely, the thickness of the PRC slab must be 60% or more of that for a jointed concrete pavement in accordance with the design guide (ACI 1988), and the slab must be of a size suitable for carrying on the roads. Further, the amount of reinforcement in a PRC slab must be determined to hold the concrete compressive stress and reinforcement tensile stress within the allowable limit against the design aircraft load. The width of cracks, which are permitted at the bottom of the slab, must be smaller than the allowable value in consideration of the durability of the slab. In addition, the structural condition of the subbase might be examined by checking the deflection caused by aircraft loading (Nagataki et al. 1997).

Cotter joint system. The use of cotter joints to connect the slabs makes it possible to increase joint rigidity. The principle of the cotter joint is that the adjacent slabs can be firmly connected by introducing compressive force at the joint. The force is realized by screwing the bolts into C-shaped cups embedded in the PRC slab through an H-shaped wedge, as shown in Figure 1, and its magnitude increases with the torque screwing the bolts. This prevents the H-shaped wedge coming loose under repeated aircraft loading, and yet the wedge is easily removed if certain slabs suffer damage.

The design method used for the cotter joint may also follow that for dowel joints in concrete pavements, as described in the structural design guide for airport pavements (MOLIT 2001, Yoder 1959). A detailed study would be necessary in advance, however, as such joints have never been applied to airports. Further, a standard work process should be established.

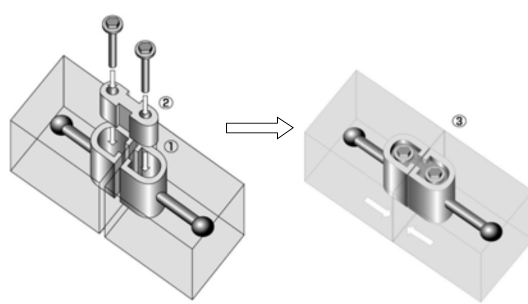

Figure 1. Schematic explanation of cotter joint system.

Laboratory tests on cotter joint system

A preliminary investigation of the effectiveness of the cotter joint system is carried out using small specimens in the laboratory. Both the bending and shearing characteristics of the cotter joint system are compared with those of conventional bolting, as generally used to connect adjoining precast segments in tunnels, buildings, and other structures.

Bending test at joint. To analyze bending characteristics at a joint, the loading test illustrated in Figure 2 was used to investigate a test piece consisting of two PRC slabs connected using two joint units. During the loading test, deflections, concrete strains, joint openings, and H-shaped wedge strain were measured.

Figure 3 gives the results of this test in the form of the relationship between bending moment and rotation angle at the joint. The test piece with the cotter joints exhibits linear elastic behavior until the stress of the H-shaped wedge reaches the allowable limit, expressed as a bending moment of 34.8 kN·m. On the contrary, the specimen with bolted joint does not have a linear relationship.

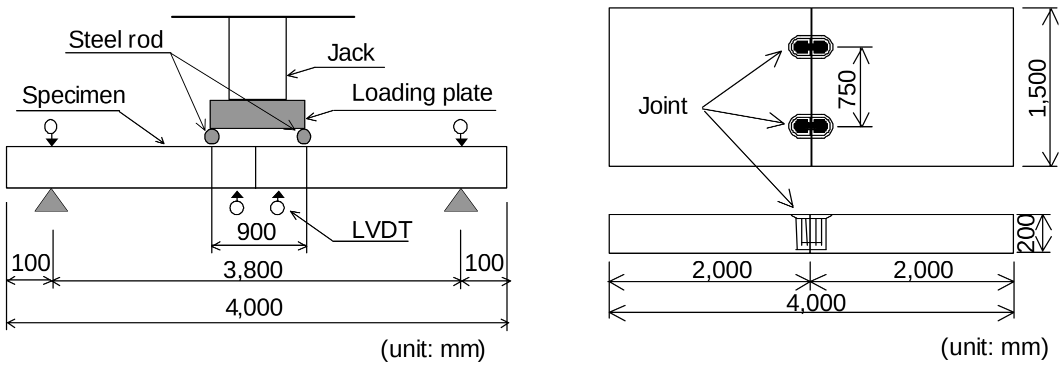

a) Test method **b) Specimen**

Figure 2. Bending test for joint system.

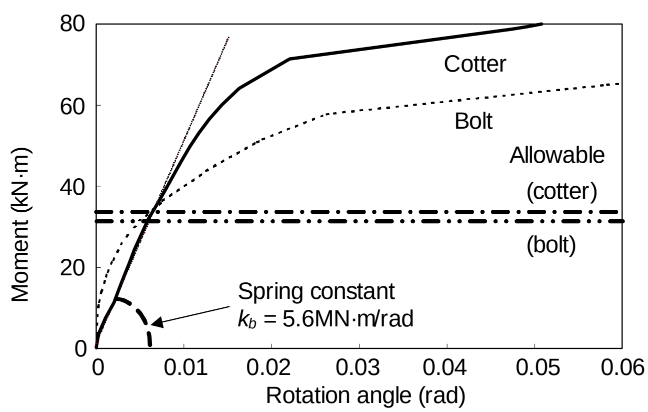

Figure 3. Bending moment and rotation angle at joint.

Shearing test at joint. As well as the bending characteristics, the shearing characteristics at the joint were studied using the loading apparatus shown in Figure 4. Here, the test piece consists of three slabs connected using two joint units. In the loading test, deflections, concrete strains, and H-shaped wedge strain were measured until failure of the joint.

The differential deflection across a joint varies with the load as shown in Figure 5. In the test piece with cotter joints, the differential deflection increases linearly with loading, even beyond the allowable stress of the H-shaped wedge. In contrast, the test piece with bolt joints exhibits tri-linear behavior.

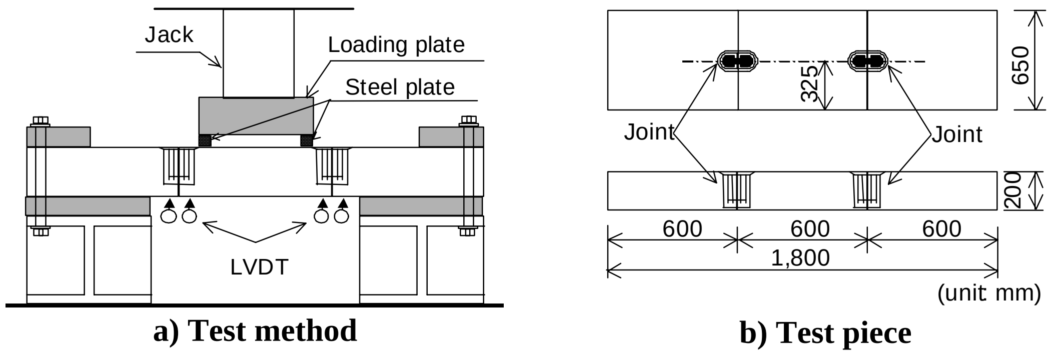

Figure 4. Shearing test for joint system.

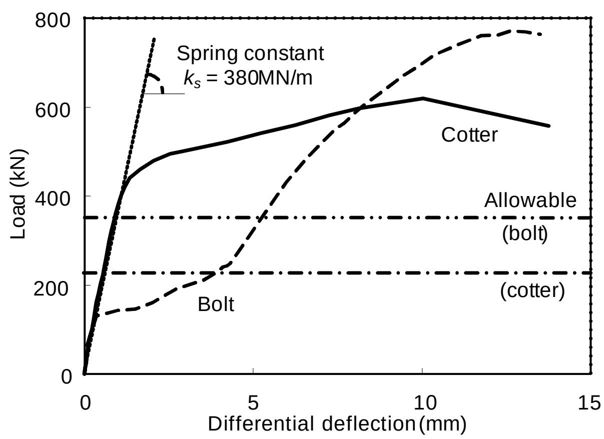

Figure 5. Differential deflection at joint.

Laboratory tests on PRC slab

To analyze the behavior of the PRC slab, the bending test shown in Figure 6 was carried out, in which deflections and strains of both concrete and reinforcement were measured. The PRC slab was 2 m in width, 4.5 m in length and 200 mm in thickness. The amount of reinforcement in the PRC slab specimen was determined in accordance with the above procedure based on allowable concrete and reinforcement stress.

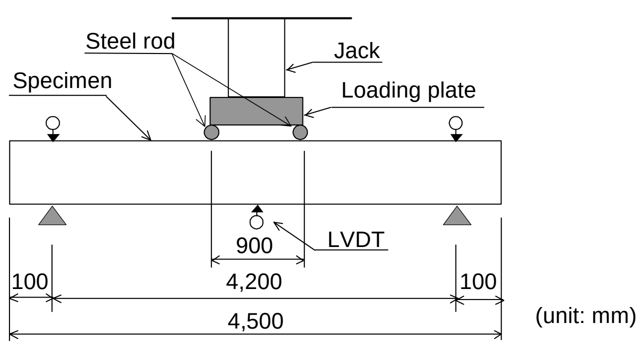

Figure 6. Bending test of PRC slab.

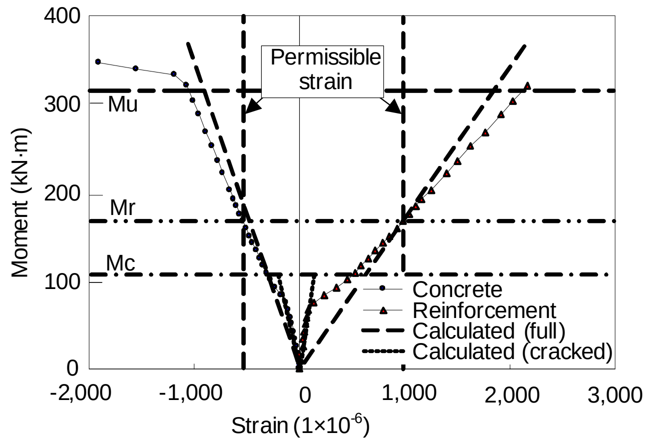

Figure 7. Concrete and reinforcement strains.

The test results are given in Figure 7, which shows the relationship between bending moment and strain for both concrete and reinforcement. Strain is calculated for both the presence and absence of cracks; denoted as cracked, full, respectively, in the figure. The measured strains coincide well with theoretically derived values up to crack occurrence, or the point at which cracks are detected visually, and remain within the elasticity limit until the reinforcement stress reaches the allowable.

Design procedure for PRC slab pavements

On the basis of the laboratory test results, we consider a design procedure for PRC slab pavements in the sections that follow.

Bending moment of PRC slab. First of all, the maximum bending moment of the PRC slab caused by the design aircraft load needs to be determined. The three-dimensional finite element method (3-D FEM) is used to analyze the behavior of the PRC slab pavement under the aircraft load. The size of linked PRC slabs is limited not to increase excessively the tensile stress due to temperature changes. Thus, the model used consists of fifty-five PRC slabs interlinked by cotter joints and resting on a subbase with a reaction coefficient of 70 MN/m^3. Each slab measured 3.5 m in width, 7.5 m in length, and 200 mm in thickness. The compressive strength, elastic modulus, and Poisson's ratio of the concrete were set at 60 MPa, 35 GPa and 0.2, respectively. Each cotter joint was modeled using both a rotating spring and a shear spring. The constant of the rotating spring, defined as the quotient of bending moment divided by rotation angle, was obtained as 5.6 MN·m/rad from Figure 3. The constant of the shear spring was calculated as 190 MN/m from Figure 5. The design aircraft load was applied at the center of the model pavement.

The maximum bending moment of a PRC slab was found to be 35.1 kN·m in the analysis, and this coincides well with the value calculated by Westergaard's equation for interior loading conditions (Westergaard 1948). This demonstrates that the maximum PRC slab stress under the design aircraft load can in practice be calculated using Westergaard's equation.

Allowable stress-based design. Three values of bending moments, read from Figure 7, are shown in Table 1. The measured value coincides well with the calculated one at the allowable stress of the reinforcement, which verifies the validity of the design procedure adopted here. The measured moment at crack occurrence is, however, smaller than the calculated one. This may indicate that the concrete tensile strength should be used in the consideration of crack occurrence in thinner concrete panels, rather than flexural strength. In conclusion, the allowable stress-based design procedure proposed for PRC slabs is proven valid.

Table 1. Bending moment of PRC slab.

Moment*	Measured	Calculated
M_c	76.5	104.4
M_r	166.4	167.9
M_u	377.4	315.4

(unit: kN·m)

* M_c: at crack occurrence, M_r: at allowable stress of reinforcement, and M_u: at ultimate failure.

Cotter joint spacing. In the case of dowel bar joints, the dowel spacing is determined using the following equation, in which the load transferred across the joint by one dowel is a function of the length and allowable tensile stress of the dowel, the allowable compressive stress of the concrete, and the joint width. In this equation, 0.4 is generally used as *α,* which means that 40% of the design load is transferred across the joint (Bradbury 1932, MOLIT 2001)

$$S = \frac{1.8 \cdot l \cdot P_a}{\alpha \cdot P} \tag{1}$$

where, S: dowel spacing, l: radius of stiffness, α: load-transfer efficiency, P_a: load transferable by one dowel, and P: design load.

In applying this equation to cotter joints, the load that one cotter joint can transfer must first be quantified. In the shearing test described above, the cotter joints failed terminally when loading reached 315 kN per joint, whereas the elastic limit is considered to be 200 kN per joint. Further, the results of both bending and shearing tests indicate that the load-transfer efficiency of cotter joints can be expected to be higher than that of bolt joints. This is, however, based on laboratory tests in which the test piece support conditions were greatly different from actual site conditions, so it must be confirmed through a prototypical experiment.

Size of H-shaped wedge and C-shaped cup. As temperature decreases, an axial tensile force acts on the cotter joint due to friction between the PRC slab and subbase. However, the joint will not open unless this tensile force exceeds the axial compressive force introduced by tightening the bolts through the H-shaped wedge to the C-shaped cups.

The size of the H-shaped wedge is checked to ensure that stress remains within the allowable limit using this equation.

$$\sigma_H = \sigma_f \cdot A_{CH} / A_H < 190 \text{ MPa} \tag{2}$$

where, σ_H: tensile stress on H-shaped wedge as a result of axial tensile force, σ_f: tensile stress due to friction between PRC slab and subbase as temperature decreases, A_{CH}: concrete cross section per cotter joint, defined as the product of joint unit spacing and slab thickness, and A_H: cross section of H-shaped wedge.

The length of the C-shaped cup is checked using this equation.

$$L_C = \frac{N_H}{\sigma_{bok} \cdot l_{sa}} \tag{3}$$

where, L_C: length of C-shaped cup, N_H: axial tensile force acting on H-shaped wedge, σ_{bok}: bonding strength of concrete, and l_{sa}: perimeter of C-shaped cup.

Loading test on experimental pavement

The design procedure for PRC slabs and cotter joints is examined by constructing an actual PRC slab pavement and observing its behavior under repeated loading equivalent to the landing gear of the design aircraft.

Outline of experimental pavement. The experimental PRC slab pavement consists of six PRC slabs connected by cotter joints. It was designed in accordance with the above-described laboratory test results and the conclusions drawn from them. The aircraft and traffic volume adopted for design purposes are a B747-400 and 20,000 coverages, respectively.

The experimental pavement consisted of PRC slabs 250 mm in thickness resting on a cement-treated subbase also 250 mm thick, as shown in Figure 8. The PRC slabs, which were manufactured in a factory, measure 2,493 mm in width, 4,493 mm in length, and 250 mm in thickness. Concrete compressive strength is 60 MPa and reinforcing steels measuring 13 mm and 16 mm in diameter are arranged at 75 mm intervals towards the top and bottom, respectively.

Four different joint structures were tested, as shown in Table 2; that is, three types of cotter joint and a removable dowel bar joint. The cotter joints consist of three combinations of bolt torque and joint unit spacing. The amount of torque was set by limiting the bolt stress to 30% and 60% of the allowable tensile stress for joint A-C joint and for joints B-D and C-E, respectively. Details of the joint structures are shown in Figure 9. The tensile strength of the C-shaped cup and the H-shaped wedge is 900 and 500 MPa, respectively.

Construction of experimental pavement. The experimental PRC slab pavement was constructed as follows. First, the cement-treated subbase was placed to a thickness of 250 mm after removing the existing layers to a depth of about 520 mm. The coefficient of foundation reaction with a loading plate of 300 mm in diameter, measured the next day, was 307 MN/m^3.

Next, the six PRC slabs were placed on a plastic film laid over the subbase. The PRC slabs were positioned both in the horizontal plane and vertically, and then the voids beneath the slabs and the joint openings were grouted and filled with cement slurry.

Finally, the PRC slabs were connected using the cotter joint system and caps were fitted to the cotter joint holes. The removable dowel bars were similarly installed at joint D-F.

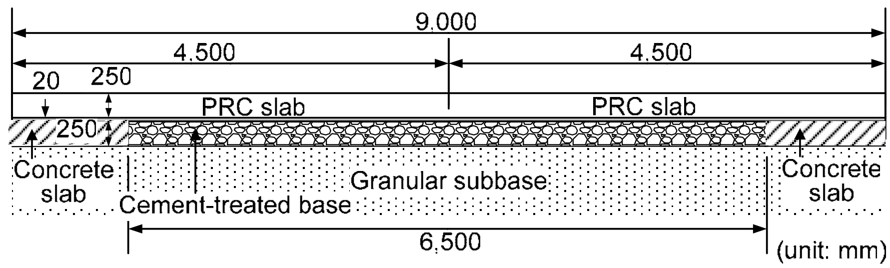

a) Section

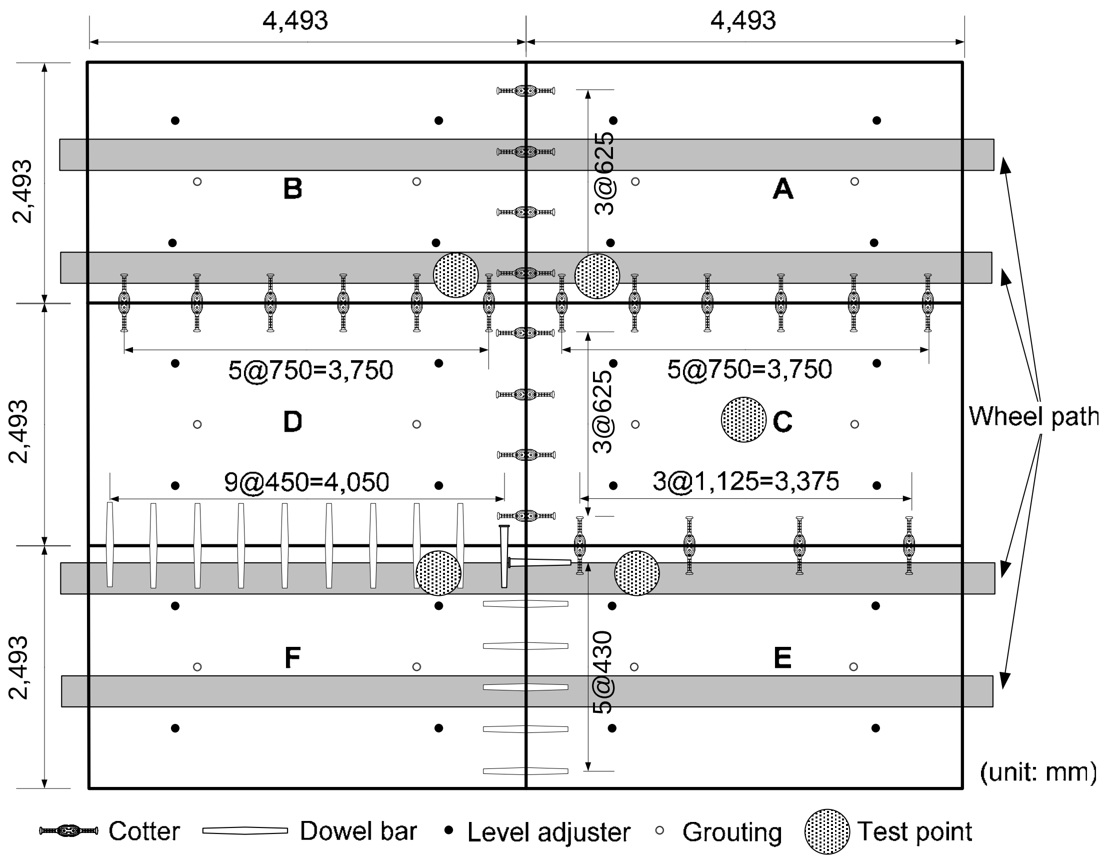

b) Plan

Figure 8. Experimental PRC slab pavement.

Table 2. Joint structures used in experimental pavement.

Section	Joint	Spacing (mm)	Torque (kN·m)
A-C	Cotter	750	200
B-D	Cotter	750	400
C-E	Cotter	1,125	400
D-F	Dowel bar	450	-

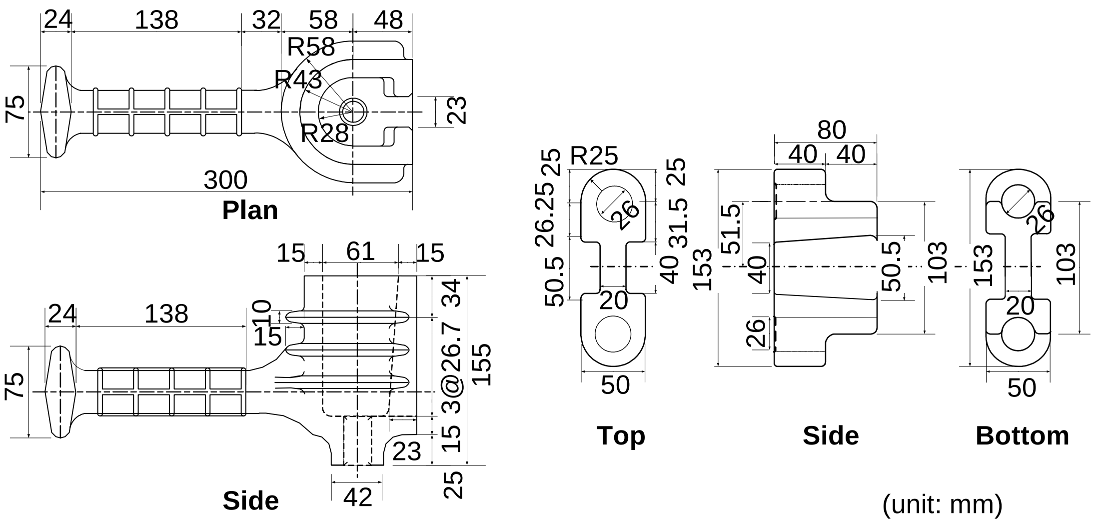

a) C-shaped cup **b) H-shaped wedge**

Figure 9. Details of cotter joint.

Loading test. Loading tests were conducted with the twin aims of determining the optimum bolt torque for the cotter joints and examining the behavior of the PRC slab pavement under aircraft loading; that is, joint tightening tests and pavement loading tests were implemented.

Joint tightening test. During the process of experimental pavement construction, the joint tightening test was carried out before fitting caps to the joints. Strains were measured on the bolt, H-shaped wedge, and PRC slab around the joint unit while increasing the torque on the bolt securing the cotter joint. This test was carried out on the cotter joint unit at the center of the PRC slab edge.

Pavement loading test. The pavement loading test entailed static loading using loading apparatus in the form of aircraft landing gear, dynamic loading using a falling weight deflectometer (FWD), and repeated loading with multiple passes of the aircraft landing gear. The groundwater level was adjusted to the mid-depth of the PRC slab; that is, the groundwater surface was 125 mm below the pavement surface.

In the static loading test, a load was applied statically through a circular plate at four joints. The loading plate, 450 mm in diameter and finished with hard rubber beneath, was placed between the joint units, and the load was increased up to a maximum of 276 kN. This loading test was conducted prior to repeated loading and again after 3,000 and 10,000 cycles of repeated loading. Deflection, joint width at top and bottom, and the strain of the concrete, reinforcement, H-shaped wedge, and bolt were measured during the test.

The dynamic loading test was carried out at the same positions as the static loading test using a FWD, having the loading plate 450 mm in diameter, with impulsive loads of 100, 150, 200 and 250 kN. This test was conducted prior to and after 1,000, 3,000, 5,000 and 10,000 cycles of repeated loading.

In the repeated loading test, the self-powered loading device modeling the landing gear of a B747 ran along the longitudinal joints up to 10,000 times. Velocity was 5 km/h and the load was 910 kN. At certain specific times, as noted above, static loading, dynamic loading, and visual observations of the surface were carried out.

Verification of PRC slab pavements

Limiting joint tightening torque. Figure 10 shows how the concrete surface strain changes with increasing bolt torque in the cotter joint along the slab edge between slabs B and D. Although strain rapidly increases until the torque reaches 150 kN·m, afterwards the increasing rate falls off.

In Figure 11, the relationship between cotter bolt torque and stress calculated from the strain of the H-shaped wedge is illustrated, with both allowable tensile stress σ_{sa} and yield stress σ_{sy} of the H-shaped wedge also shown. The curve changes at a torque of about 250 kN·m, when the tensile stress reaches the allowable tensile stress.

Within the elastic range, this relationship can be expressed by the following equation. That is, the tightening force on the cotter joint bolt can be easily controlled by the torque.

$$T = 1.3 \times 10^3 \sigma_s \quad (4)$$

where, T : bolt torque (kN·m), and σ_s : tensile stress of H-shaped wedge (MPa).

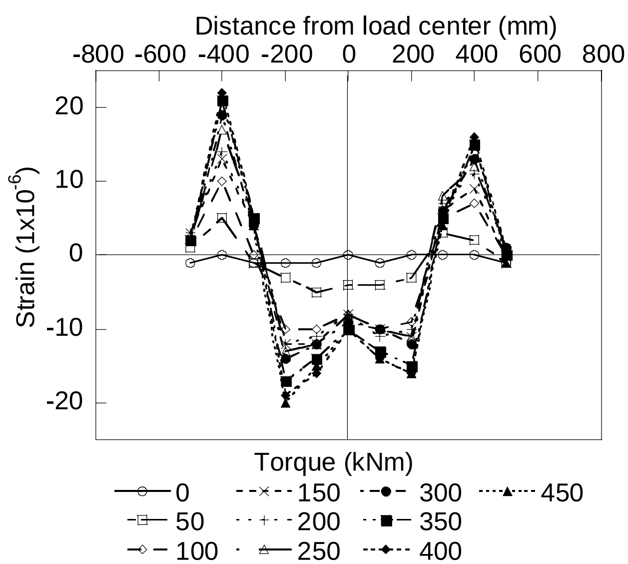

Figure 10. Changes in PRC slab strain with bolt torque.

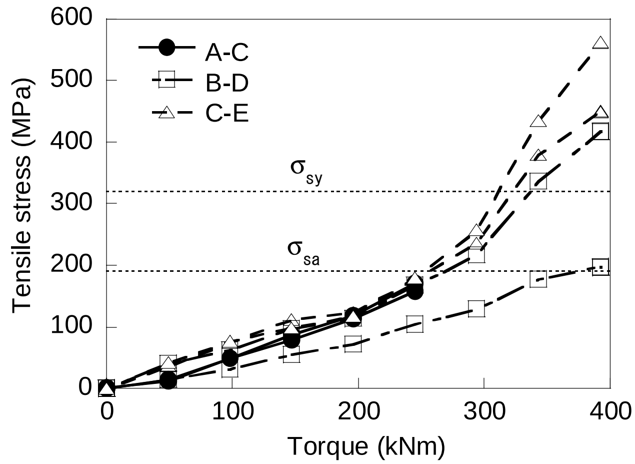

Figure 11. Change in tensile stress of H-shaped wedge with bolt torque.

Durability of PRC slab pavement. The static loading test provides results for the variation in PRC slab strain underneath the loading plate during repeated loading, as shown in Figure 12. The strain barely increases as the number of loading cycles rises, demonstrating that the PRC slab has sufficient bearing capacity to sustain repeated loading.

From the results of the dynamic loading test, Figure 13 shows the change in maximum deflection D_0 over the course of the repeated loading test, indicating that D_0 remains almost constant with increasing number of cycles. This demonstrates that the load-carrying capacity of the subbase and subgrade changes little with load repetition, even if the PRC slab pavement is almost soaked in water.

During the repeated loading test, cracks were first detected in the PRC slab at 5,000 cycles, and the number of cracks gradually increased. The state of cracking at 10,000 loading cycles is shown in Figure 14. Most cracks originated from grout injection holes, cotter joints, and so on, especially in slab B. As for the crack width, most were 0.06 mm or less at 5,000 cycles and 0.08 mm or less at 10,000 cycles, so the crack width barely increases with loading.

Cracks were also detected in slabs C and D although the loading apparatus did not run directly over these. Supposing that these were associated with the negative bending moment in the interior of the PRC slabs, the stress condition of PRC slabs was analyzed using 3-D FEM. The maximum stress was found to be 2.0 MPa, which could cause cracks initiation from grout injection holes, etc., although it is below the allowable stress.

The influence of cracks on the durability of PRC slab was examined in accordance with the procedure specified by the Japan Society of Civil Engineers (Nagataki et al. 1997). In comparison with the 0.2 mm maximum crack width specified by the JSCE under normal environmental conditions, the observed width of 0.08 mm is satisfactorily small. Further, the influence of cracking on the bottom of the PRC slabs was examined by estimating the crack width from the maximum reinforcement stress in slab C. Here, a maximum crack width of 0.05 mm was obtained from the maximum stress of 21 MPa at 276 kN loading, which is smaller than the designed crack width of 0.088 mm. Therefore, the durability of PRC slab is proven to be sufficient under this loading condition.

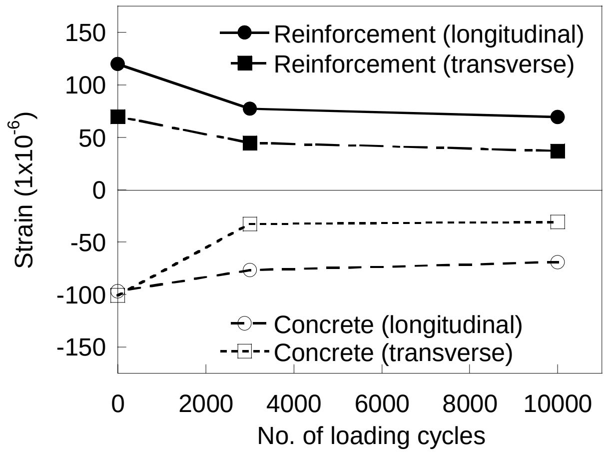

Figure 12. Variation in strain during repeated loading test.

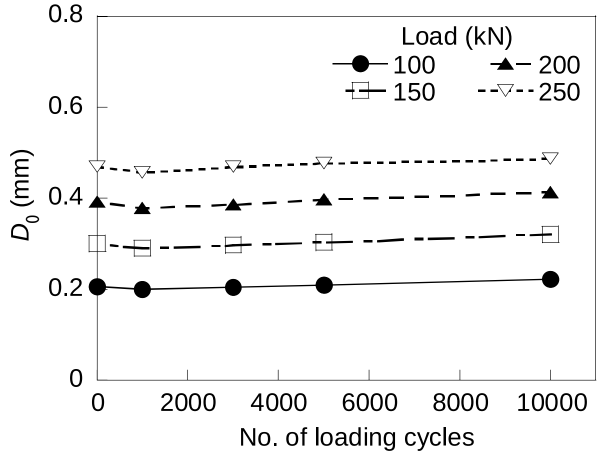

Figure 13. Variation in FWD maximum deflection during repeated loading test.

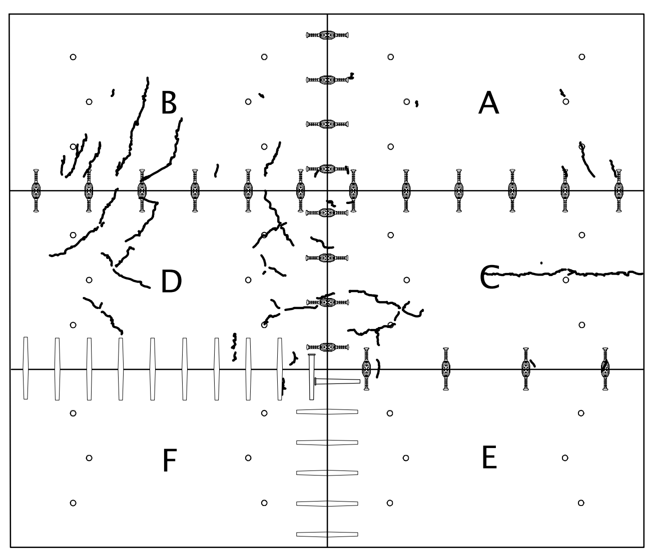

Figure 14. Cracks in PRC slab after repeated loading test.

Durability of cotter joint. The results of the static loading test at a joint are presented in Figure 15, which shows the joint spread at top and bottom when a load of 276 kN was applied between the joints. This demonstrates that the bending moment is fully transmitted through the cotter joint, because the cotter joint closes at the top and opens at the bottom, respectively, in contrast with the dowel bar joint (D-F).

The variation in joint spread between slabs A and C with repeated loading is explained in Figure 16. As the repeated loading test proceeded, the joint remains closed at the top and open at the bottom, respectively, and the gradient is constant through the thickness of the slab. Thus, the cotter joint proves to have sufficient durability against repeated loading up to this extent.

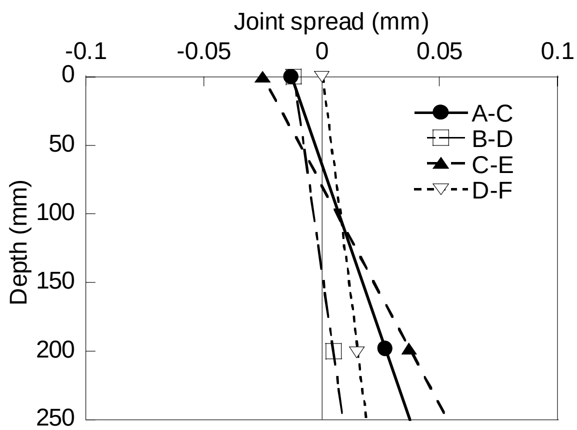

Figure 15. Joint spread at various joints.

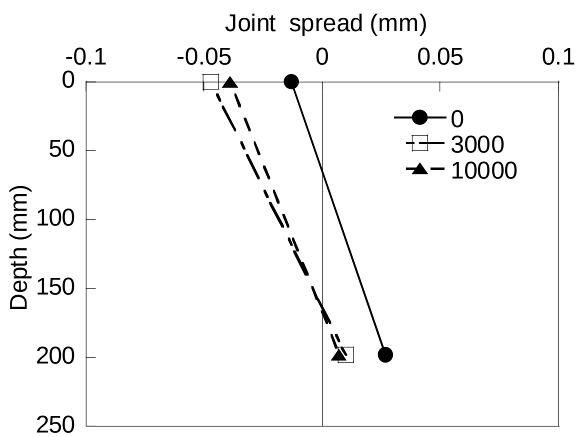

Figure 16. Changes in joint spread during repeated loading.

The efficiency of load transfer at joint E_f, as defined by the following equation, was calculated from the deflections measured in the dynamic loading test with FWD (Yamanoi et al. 1991).

$$E_f = \frac{D_{450} / \{(D_{450} + D_0)/2\}}{D'_{450} / \{(D'_{450} + D'_0)/2\}} \times 100 \qquad (5)$$

where, D_0, D_{450}: deflection measured at joint, and D'_0, D'_{450}: deflection measured in the interior. The suffices represent distance from the load center. As the loading plate is placed adjacent to the slab edge in the former, D_0, D_{450} is a deflection of 225 mm apart from joint at loaded, non-loaded slab, respectively.

Figure 17 shows the changes in load-transfer efficiency at various joints during the repeated loading test. For all joints, load-transfer efficiency barely changes, retaining a value of 90% or more up to 10,000 loading cycles, although it decreases to some extent in the initial stage. However, the load-transfer efficiency at joints where the spacing is 1,125 mm decreases after 5,000 cycles (C-E). On the contrary, where the spacing is 725 mm (A-C and B-D), the load-transfer efficiency remains above 96%, equivalent to the value for the dowel bar joint (D-F). Thus, the spacing of cotter joint units should be made 750 mm.

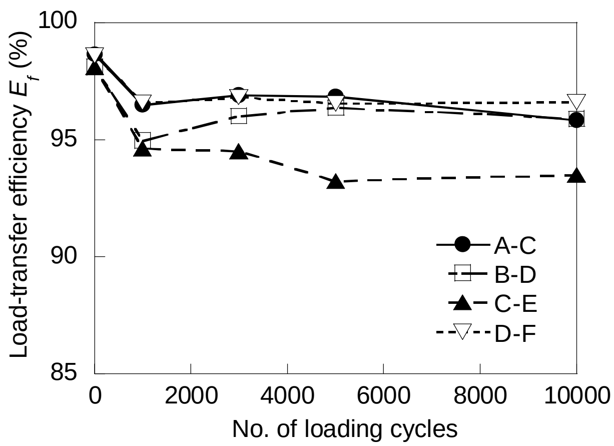

Figure 17. Comparison of load-transfer efficiency at various joint.

Conclusions

A pavement system consisting of precast reinforced concrete (PRC) slabs of high-strength concrete connected with cotter joints was studied in laboratory tests and through construction of an experimental pavement. This work verified the applicability of PRC slab pavements with cotter joints to airports. The main findings are listed below.

Cotter joints.

1) Since the tensile stress of the H-shaped wedge reaches its allowable limit stress at a bolt torque of 250 kN·m, the torque should be limited to 250 kN·m or less.
2) The load-transfer efficiency at cotter joints with a cotter spacing of 1,125mm is less than that at a spacing of 750 mm, so the cotter spacing should be standardized at 750 mm.
3) Since a cotter joint designed in accordance with the above maintains a load-transfer efficiency of 96%, the proportion of the design load transferred to the next slab through the joint is 48%.

PRC slabs.

1) The measured maximum bending moment of a PRC slab connected using cotter joints is equivalent to that calculated by Westergaard's equation, so the maximum bending moment can be easily determined using the equation.
2) The measured bending moment of a PRC slab is equivalent to the calculated value, so the conventional allowable stress-based design procedure can be applied.
3) The concrete and reinforcement strains, and also the deflection, barely change during repeated loading, so the bearing capacity of a PRC slab pavement designed in accordance with the design guide for airport pavements proves sufficient.

The PRC slab pavement described here was implemented at Fukuoka Airport in 2004, after some improvements to the shape of the H-shaped wedge and introducing fiber reinforced concrete at the surface portion of the PRC slab to prevent cracks from occurring.

References

American Concrete Institute (ACI) (1988). "Recommendations for designing prestressed concrete pavements", *ACI Structural Journal*, July - August, pp.451-471.

Bradbury, R.D. (1932). "Design of joints in concrete pavements", *Proc., Highway Research Board*, Vol.12, pp.105-136.

Hachiya, Y., Akamine, F., Takahashi, O., Miyaji, Y. (2001). "Rapid repair with precast prestressed concrete slab pavements using compression joint system", *Proc.*, *7th International Conference on Concrete Pavements*, pp.891-905.

Ministry of Land, Infrastructure and Transport (MOLIT) (2001). *Design guide for airport pavements*, 147p. (in Japanese).

Nagataki, S., Kasahara, A., Sato, R., Hachiya, Y. (1997). "Serviceability based concrete pavement design - JSCE methods", *Proc.*, *6th International Conference on Concrete Pavement Design and Materials for High Performance*, Vol.1, pp.23-37.

Sato, K., Fukute, F., Inukai, H. (1981). "Some new construction methods for prestressed concrete airport pavements", *Proc.*, *2nd International Conference on Concrete Pavement Design,* pp.149-159.

Westergaard, H. M. (1948). "New formulas for stresses in concrete pavements of airfields", *Transaction of ASCE*, Vol.113, pp.425-444.

Yamanoi, A., Kawakami, A., Ogishima, T., Miyamoto, T., Watanabe, N. (1991). "Evaluation of load transfer efficiency of RCCP", *Proc., 46th Annual Meeting of Japan Society of Civil Engineers*, Section V, pp.128-129. (in Japanese).

Yoder, E. J. (1959). *Principles of pavement design*, John Wiley & Sons.